Molecular Mass Growth Processes to Polycyclic Aromatic Hydrocarbons through Radical–Radical Reactions Exploiting Photoionization Reflectron Time-of-Flight Mass Spectrometry

Shane J. Goettl,[1] Musahid Ahmed,[2]* Alexander M. Mebel,[3]* Ralf I. Kaiser,[1]*

[1]*Department of Chemistry, University of Hawai`i at Mānoa, Honolulu, HI 96822*

[2] *Chemical Sciences Division, Lawrence Berkeley National Laboratory, Berkeley, CA 94720*

[3] *Department of Chemistry and Biochemistry, Florida International University, Miami, FL 33199*

ralfk@hawaii.edu

CONSPECTUS: Polycyclic aromatic hydrocarbons (PAHs) represent critical building blocks in molecular mass growth processes to carbonaceous nanoparticles, referred to as interstellar and circumstellar grains along with soot particles in astrophysical environments and combustion systems, respectively. Recent advancements on elucidating elementary steps to PAHs have utilized reactions of aromatic radicals, resonantly stabilized free radicals, and aliphatic radicals with closed shell hydrocarbons. However, the role of radical–radical reactions (RRR) leading to PAHs has remained largely unexplored on the molecular level due to preceding experimental challenges in producing sufficiently high number densities of radical reactants for isomer-selective detection of products from bimolecular and termolecular reactions. This *Account* offers the latest developments in our knowledge on the mechanisms and pathways to PAHs via RRR probed in a chemical microreactor at temperatures as high as 1,500 K. Product preservation in a molecular beam coupled with synchrotron vacuum ultraviolet photoionization reflectron time-of-flight mass spectrometry and photoelectron photoion coincidence spectroscopy enabled isomer-selective detection of PAHs of up to three rings by their photoionization efficiency curves, which were fit with a linear combination of reference curves for identification. Experiments were combined with computational fluid dynamics modeling of the physico-chemical processes in the microreactor, as well as high-level electronic structure calculations to reveal the reaction pathways of each system. Six distinct reaction mechanisms were discovered in this work: Propargyl Addition – BenzAnnulation (PABA), Methyl Addition – Ring Expansion (MARE), CycloPentadienyl Addition – Naphthylization (CPAN), Fulvenallenyl Addition – Cyclization – Aromatization (FACA), Benzyl Addition – Aromatization (BAA), and Phenyl Addition – Pentacyclization (PAP). By systematically varying the number of carbon atoms in the radical reactants, molecular mass growth processes involving reactions between radicals with odd numbers of carbon atoms access aromatics carrying one, two, or three six-membered rings, whereas reactions between even- and odd-carbon-numbered radicals produce aromatics combining five- and six-membered rings. Our investigations reveal unconventional cycloadditions on excited state triplet surfaces, additions of radicals to low spin density carbon-centered radicals, spiroaromatic and fulvene-type intermediates, and highly strained bicyclic reaction intermediates, challenging current perceptions of PAH molecular mass growth processes. All the listed mechanisms, except for FACA, feature endoergic reactions or barriers which lie above the separated reactants and therefore might be

central to circumstellar environments of carbon-rich stars and planetary nebulae as their descendants, but they play no role in the gas phase of cold molecular clouds where temperatures as low as 10 K dominate. Overall, this work provides detailed reaction mechanisms of PAH growth processes, advancing our knowledge of the chemistry of carbonaceous matter in the universe.

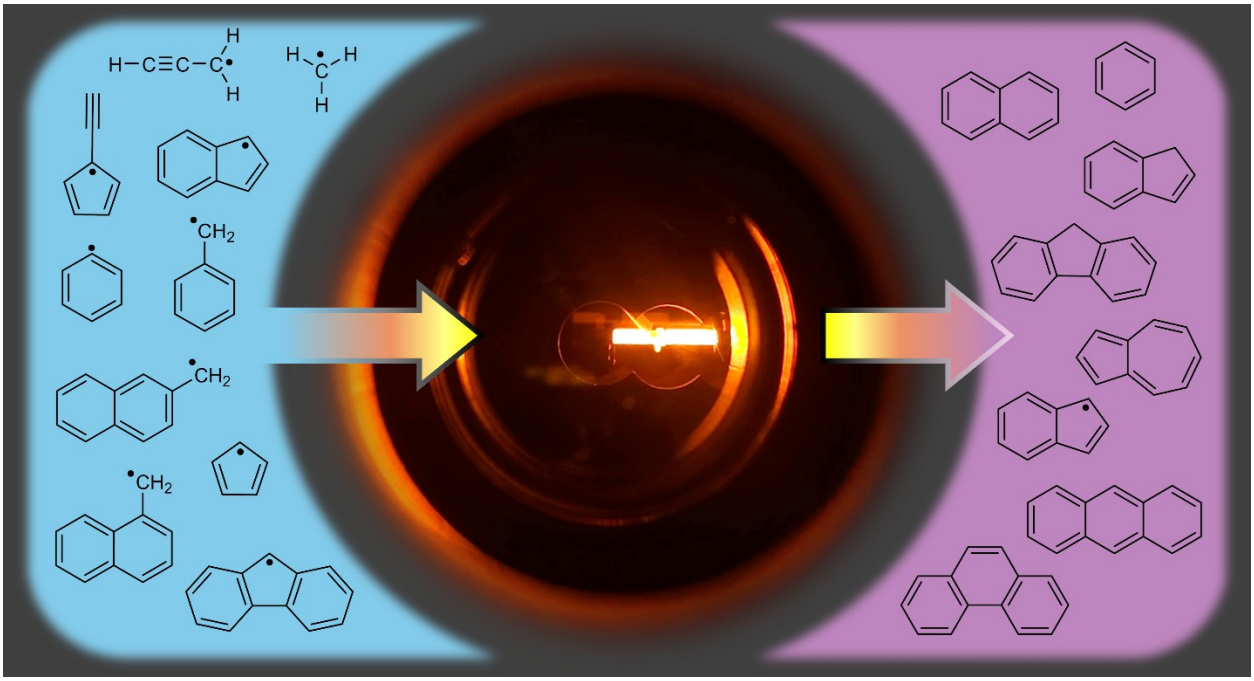

KEY REFERENCES:

- He, C.; Kaiser, R. I.; Lu, W.; Ahmed, M.; Krasnoukhov, V. S.; Pivovarov, P. S.; Zagidullin, M. V.; Azyazov, V. N.; Morozov, A. N.; Mebel, A. M. Unconventional gas-phase preparation of the prototype polycyclic aromatic hydrocarbon naphthalene ($C_{10}H_8$) via the reaction of benzyl (C_7H_7) and propargyl (C_3H_3) radicals coupled with hydrogen-atom assisted isomerization. *Chem. Sci.* **2023**, *14*, 5369.[1] *This experimental investigation combined with computational fluid dynamics (CFD) and kinetic modeling explores the Propargyl Addition – BenzAnnulation (PABA) mechanism, where reactions of astronomically abundant propargyl radicals with ylomethyl-substituted aromatics yield naphthalene moieties and highlight the significance of hydrogen-assisted isomerization.*
- Kaiser, R. I.; Zhao, L.; Lu, W.; Ahmed, M.; Zagidullin, M. V.; Azyazov, V. N.; Mebel, A. M. Formation of benzene and naphthalene through cyclopentadienyl-mediated radical–radical reactions. *J. Phys. Chem. Lett.* **2022**, *13*, 208.[2] *The importance of five-membered ring expansion in circumstellar environments and combustion processes is showcased via the CycloPentadienyl Addition – Naphthylization (CPAN) mechanism through the cyclopentadienyl radical self-reaction forming naphthalene, essentially converting two five-membered rings into two fused six-membered rings.*
- Kaiser, R.; Zhao, L.; Lu, W.; Ahmed, M.; Krasnoukhov, V. S.; Azyazov, V. N.; Mebel, A. M. Unconventional excited-state dynamics in the concerted benzyl (C_7H_7) radical self-reaction to anthracene ($C_{14}H_{10}$). *Nat. Commun.* **2022**, *13*, 1.[3] *The [3+3] cycloaddition on the excited-state surface in the benzyl radical self-reaction opens up the Benzyl Addition – Aromatization (BAA) mechanism as an avenue for rapid synthesis of multi-ringed structures through excited-state gas-phase dynamics in a thermal reaction.*
- He, C.; Kaiser, R. I.; Lu, W.; Ahmed, M.; Pivovarov, P. S.; Kuznetsov, O. V.; Zagidullin, M. V.; Mebel, A. M. Unconventional pathway in the gas-phase synthesis of *9H*-fluorene ($C_{13}H_{10}$) via the radical–radical reaction of benzyl (C_7H_7) with phenyl (C_6H_5). *Angew. Chem., Int. Ed.* **2023**, *62*, e202216972.[4] *The Phenyl Addition – Pentacyclization (PAP) mechanism as shown here by the reaction of benzyl with phenyl provides a unique view of how aromatic radical–radical reactions need not proceed through recombination of their radical centers.*

1. INTRODUCTION

The first isolation of naphthalene ($C_{10}H_8$) from distillation of coal tar by Garden in 1820[5] led to the discovery of polycyclic aromatic hydrocarbons (PAHs)—organic molecules carrying fused benzene rings. Subsequently, PAHs have emerged as fundamental molecular building blocks and precursors to carbonaceous nanostructures[6,7] involving bottom-up molecular mass growth processes in high- and low-temperature environments. These nanostructures, often referred to as soot particles in combustion settings (1,000–2,000 K),[8] are known as interstellar and circumstellar grains in molecular clouds (10 K)[9] and carbon-rich envelopes of evolved asymptotic giant branch (AGB)[10] stars with temperatures of up to a few 1,000 K, respectively. Planar PAHs such as coronene ($C_{24}H_{12}$, **1**) along with two-dimensional nanostructures (graphenes, nanoflakes) require six-membered rings as present in the benzene moiety [benzene (C_6H_6, **4**)] (Figure 1). Non-planar PAHs like corannulene ($C_{20}H_{10}$, **2**) together with three-dimensional nanostructures (nanobowls, nanotubes, fullerenes) necessitate five-membered cyclic building blocks [cyclopentadiene (C_5H_6,

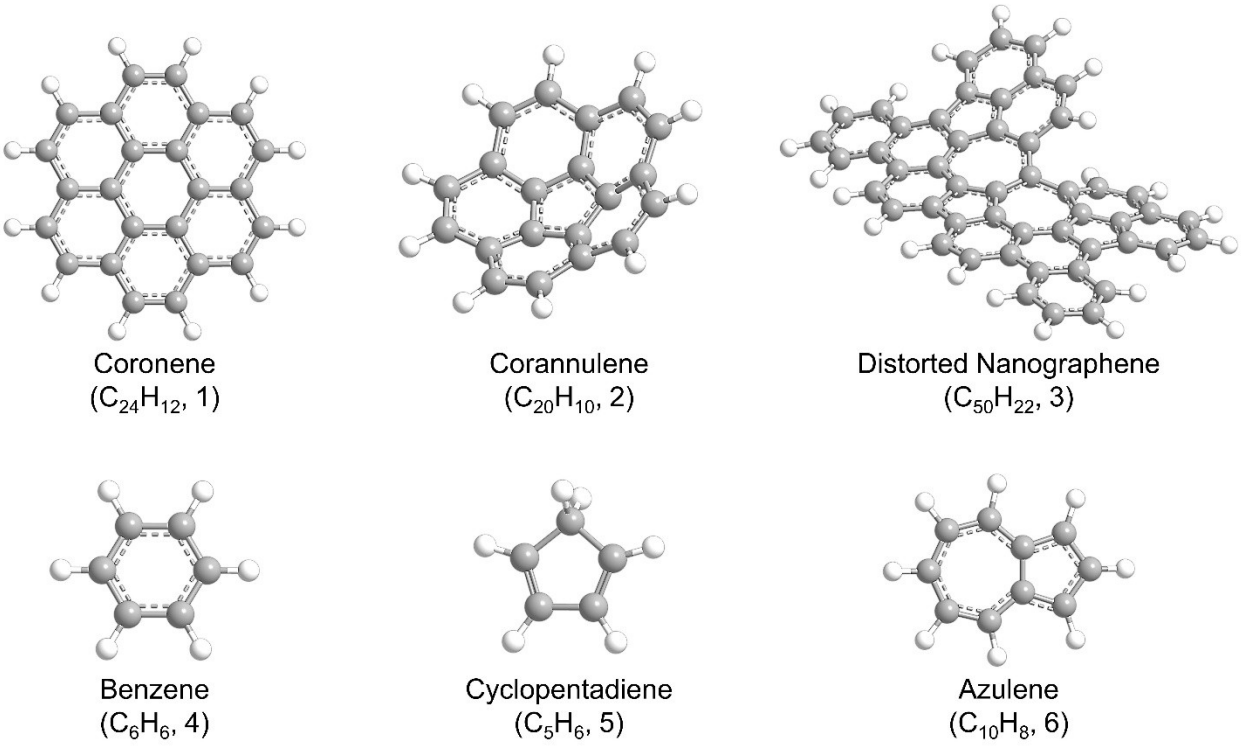

Figure 1. Prototype planar (coronene, $C_{24}H_{12}$, **1**), bent (corannulene, $C_{20}H_{10}$, **2**), and contorted (nanographene, $C_{50}H_{22}$, **3**) PAHs along with their molecular building blocks benzene (C_6H_6, **4**), cyclopentadiene (C_5H_6, **5**), and azulene ($C_{10}H_8$, **6**).

5)] to bend their planar molecular structures out of the plane. Five-membered rings annulated to a seven-membered cyclic moiety such as in distorted nanographenes (**3**) require an azulene moiety ($C_{10}H_8$, **6**) accessing contorted, saddle-shaped aromatic systems with both a positive and negative curvature of the carbon backbone.

On Earth, PAHs are ubiquitous. These aromatics are largely linked to unwanted byproducts of incomplete combustion processes of fossil fuels and biofuels in transportation and power generation as well as naturally in emissions from forest fires and volcanoes.[11] Terrestrial PAHs are typically carcinogenic and highly toxic.[12] However, in the interstellar medium, PAHs and their alkylated, ionized, (de)hydrogenated, and protonated derivatives may account for up to 30 % of the cosmic carbon budget[13,14] as derived from the analysis of diffuse interstellar bands (DIBs)[15] and unidentified infrared (UIR) emissions[16] in the ultraviolet (200–400 nm) and infrared (3–20 μm) regions of the electromagnetic spectrum, respectively, and reinforced through microwave detections of cyano-substituted PAHs with sizes ranging up to cyanocoronene.[17] In these environments, PAHs represent key intermediates and nucleation sites leading eventually to circumstellar and interstellar grains[18] through high- and low-temperature molecular mass growth processes. Furthermore, the identification of PAHs as complex as chrysene ($C_{18}H_{12}$) and triphenylene ($C_{18}H_{12}$) on the carbonaceous asteroid Ryugu[19] shows the rich chemistry that PAHs facilitate, leading to discrete pathways involving a classical high temperature synthesis in carbon-rich circumstellar envelopes, but also unexpected low-temperature pathways in molecular clouds such as TMC-1.[20]

Therefore, the fundamental understanding of the key processes and mechanisms in the synthesis of PAHs along with their precursors provides insights into how complex aromatic structures such as graphenes, fullerenes, and carbonaceous nanoparticles (soot, interstellar grains) are formed. These studies also critically assist in elucidating the formation pathways that PAHs afford to supramolecular chemistry and material sciences (optoelectronic devices, quantum dots) leading to a diverse array of carbon-based materials such as carbon nanotubes (CNTs), nanohoops, nanobelts, nanocones, cycloparaphenylenes (CPPs), polyparaphenylenes (PPPs), Möbius macrocycles, nanographenes, graphite, nanoribbons, and nanobowls. The underlying elementary steps and reaction mechanisms engaged in molecular mass growth processes to PAHs involving reactions of aromatic radicals (AR), resonantly stabilized free radicals (RSFRs), and aliphatic

radicals with closed shell hydrocarbons are captured in the **H**ydrogen **A**bstraction – C_2H_2 (acetylene) **A**ddition (**HACA**, **R1**),[21-23] **H**ydrogen **A**bstraction – **V**inylacetylene **A**ddition (**HAVA**, **R2**),[24] **P**henyl **A**ddition – dehydro**C**yclization (**PAC**, **R3**),[25-27] and **M**ethylidyne **A**ddition – **C**yclization – **A**romatization (**MACA**, **R4**)[28] mechanisms (Figure 2). However, the role of **R**adical–**R**adical **R**eactions (**RRR**) in the synthesis of aromatic structures on the molecular level have been largely elusive. This lack of knowledge is associated with the absence of sophisticated molecular beam experiments coupled with the experimental inability to prepare sufficiently high number densities of the fragile radical reactants that allow for an isomer-selective detection of the reaction products generated in successive bimolecular and/or termolecular reactions.

This *Account* presents recent advances on the gas-phase formation mechanisms of up to three-ringed aromatic hydrocarbons synthesized via previously elusive **RRR** (Figure 3) involving C1 to C13 hydrocarbon radicals (Figure 4) in a high-temperature chemical microreactor coupled with an isomer-specific identification enabled by vacuum ultraviolet photoionization reflectron time-of-flight mass spectrometry (ReTOF-MS) or photoelectron photoion coincidence spectroscopy (PEPICO) at a synchrotron.[29,30] By systematically varying the number of carbon atoms in the radical reactants, molecular mass growth processes involving reactions between two odd-numbered radicals access aromatics carrying one (benzene), two (naphthalene, $C_{10}H_8$, **7**), and three (anthracene/phenanthrene, $C_{14}H_{10}$, **10/11**) six-membered rings. Benzene was prepared in the C1–C5[2] and C3–C3[31] systems, naphthalene was formed in C1–C9,[32] C3–C7,[1,33] and C5–C5[2] reactions, and anthracene/phenanthrene were synthesized in the C1–C13,[34] C3–C11,[35] C5–C9,[36] and C7–C7[3] systems. These reactions involved the methyl (CH_3, **13**), propargyl (*C_3H_3*, **14**), cyclopentadienyl (*C_5H_5*, **15**), fulvenallenyl (*C_7H_5*, **17**), benzyl (***C_7H_7***, **18**), 1-indenyl (***C_9H_7***, **9**), 1- and 2-naphthylmethyl (***$C_{11}H_9$***, **19/20**), and 9-fluorenyl (***$C_{13}H_9$***, **21**) radicals; resonantly stabilized free radicals (RSFRs) are denoted in italics, whereas aromatic radicals (AR) are highlighted in bold (Figure 4). Those experiments were expanded systematically to the formation of aromatics carrying five- and six-membered rings [indene (C_9H_8, **8**), 1-indenyl, fluorene ($C_{13}H_{10}$, **12**)] synthesized in the C3–C6[37] and C7–C6[4] systems through reactions involving propargyl plus phenyl (**C_6H_5**, **16**) and benzyl plus phenyl radicals. This *Account* concludes with implications of our results to the often-exotic gas-phase hydrocarbon chemistries in combustion systems and

molecular mass growth processes in deep space highlighting future research directions involving PEPICO in this field.

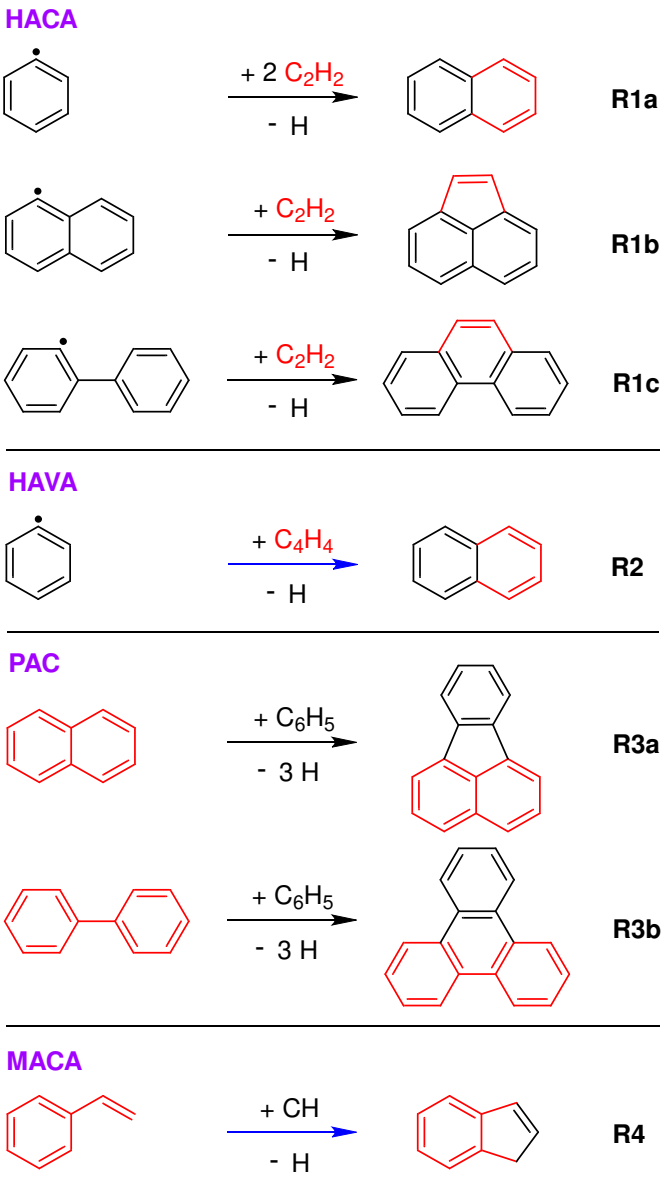

Figure 2. Fundamental pathways involved in molecular mass growth processes via **H**ydrogen **A**bstraction – C_2H_2 (acetylene) **A**ddition (**HACA**), **H**ydrogen **A**bstraction – **V**inylacetylene **A**ddition (**HAVA**), **P**henyl **A**ddition – Dehydro**C**yclization (**PAC**), and **M**ethylidyne **A**ddition – **C**yclization – **A**romatization (**MACA**). Arrows in blue indicate barrierless pathways. Building blocks color coded in red define the moieties of the closed shell reactants. At elevated temperatures, **HACA** can lead to the gas-phase synthesis of naphthalene ($C_{10}H_8$, **R1a**); [3+2] (**R1b**) and [4+2] (**R1c**) bay closures result in annulations of five- and six-membered rings, respectively. The barrierless **HAVA** route converts phenyl radicals to naphthalene via [4+2] ring annulation (**R2**). **PAC** provides high temperature routes to indene and naphthalene moieties via [6+3] and [6+4] additions as exemplified in reactions **R3a** and **R3b**. **MACA** converts vinyl substituted aromatics to indene moieties via barrierless [5+1] addition (**R4**).

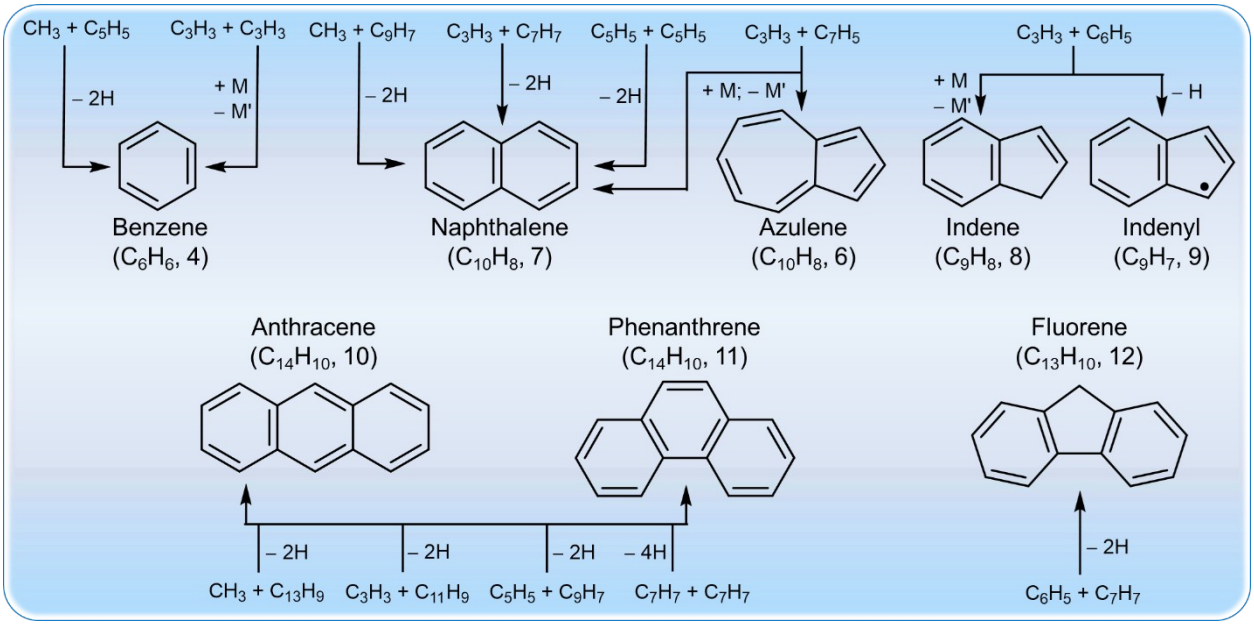

Figure 3. Pathways to aromatic hydrocarbons via gas-phase **R**adical–**R**adical **R**eactions (**RRR**)**.**

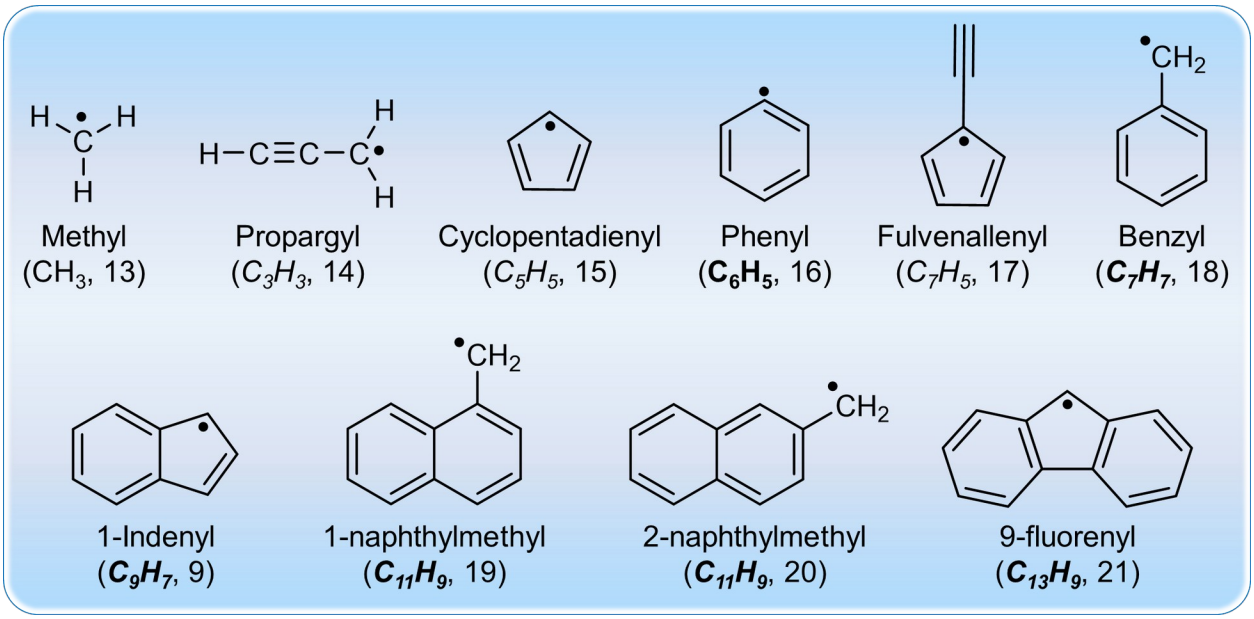

Figure 4. Structures of radical reactants exploited to synthesize aromatics with up to three rings in the gas-phase via **R**adical–**R**adical **R**eactions (**RRR**).

2. METHODOLOGY

The experiments employed here used a chemical microreactor interfaced to a molecular beam machine and either a ReTOF or PEPICO mass spectrometer in conjunction with vacuum ultraviolet (VUV) photoionization (Figure 5).[29,30] Thermally labile reactants are seeded in helium carrier gas at typical backing pressures of 100 to 600 Torr with precursor concentrations of less than 1 %. These gas mixtures are introduced through a 100–200 μm nozzle into a resistively heated silicon carbide (SiC) tube with an inner diameter of 1 mm that can be heated from 20–40 mm. Temperatures of up to 1,500 K pyrolyze the precursors, and the resulting radicals then react within the silicon carbide tube. Short residence times and dilute radical concentrations allow molecular mass growth processes to initiate through the *in situ* reaction of two radicals. The continuous supersonic beam is skimmed and interrogated in the ionization region of the ReTOF/PEPICO spectrometer by tunable, quasi-continuous (500 MHz) VUV synchrotron radiation at the Chemical Dynamics Beamline (9.0.2) of the Advanced Light Source or the X04DB Beamline of the Swiss Light Source. Time-of-flight spectra are recorded, and photoionization efficiency (PIE) curves of an ion of a well-defined mass-to-charge ratio (m/z) can be obtained by plotting the integrated ion signal at that m/z versus the photon energy, while mass-selected threshold photoelectron (ms-TPES) spectra are collected while selecting only the photoelectrons with kinetic energy less than 10 meV in coincidence with photoions at the desired m/z. These PIE curves and ms-TPE spectra are central for the identification of structural isomers via fitting with a linear combination of known reference curve(s).

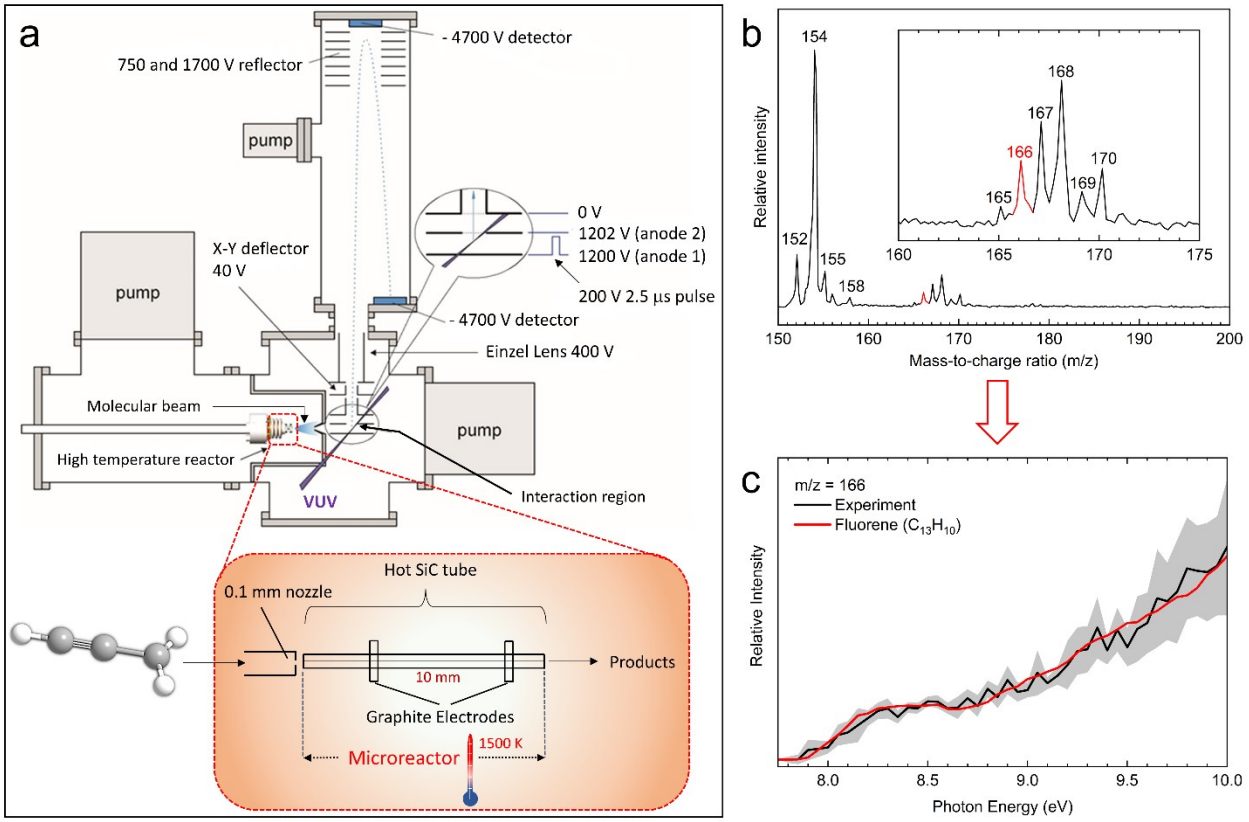

Figure 5. **(a)** Schematics of the experimental setup, **(b)** typical single photoionization mass spectrum, and **(c)** corresponding photoionization efficiency curves (PIE). In panel **(a)**, the mass spectrometer is reproduced from ref 66 with permission from the PCCP Owner Societies, while the remainder is reproduced from ref 67, copyright 2024 American Chemical Society. The spectra in panels **(b)** and **(c)** are reproduced from ref 4 with permission from Wiley.

Describing the physico-chemical processes in the microreactor requires combining computational fluid dynamics (CFD) simulations with chemical kinetics modeling.[38,39] The simulations begin with solving the electric current and heat transfer equations where the current resistively heats the microtubular SiC reactor. The released heat is transferred to the stainless steel housing and is also radiatively emitted through the outer surface of the setup, whereas the hot inner surface of the reactor heats the gas flow. Next, the Navier-Stokes equation is solved to describe gas motion in the reactor, and mass transfer equations are solved for strongly diluted components in the carrier gas. While the gas flow moves through the reactor, the mass transfer equations are coupled with chemical kinetics equations describing rates of production and consumption of the reactants, intermediates, and products involved in the reaction mechanism. The gas dynamic parameters

exhibit strong axial gradients and the CFD/chemical kinetics simulations provide the profiles of the axial gas temperature, velocity, pressure, concentrations of the species of interest and reaction rates, the gas residence time in the reactor, and the products' mole fractions on the exit from the reactor. The gas residence time in the reactor is typically in the range of 50–200 μs depending on the nature of the carrier gas and the gas flow rate. The residence time rapidly decreases with the gas flow rate when it is below 100 sccm and then drops only mildly with the flow rate in the 200 to 400 sccm range. The CFD modeling showed that using He as a carrier gas is preferable, as this allows one to achieve lowest residence times.[39]

Development of the chemical reaction mechanism inside the reactor requires a balance between high accuracy and computational demands to select an appropriate method for the electronic structure *ab initio* molecular orbital or density functional theory (DFT) calculations of a potential energy surface (PES). This balance is normally achieved by the use of dual-level calculations where geometries of reaction intermediates and transition states are optimized using DFT methods, such as ωB97XD[40,41] and B2PLYPD3,[42] and single-point energies are refined at the explicitly correlated CCSD(T)-F12[43,44] level with Dunning's correlation-consistent basis sets[45,46] or utilizing G3-type model chemistries (for larger systems).[47-49] The necessity of the use of multireference methods is monitored by the T1 diagnostic in CCSD, and the structures with multireference wavefunctions are treated using multireference perturbation theory CASPT2[50] and the spin-splitting method.[51,52] The electronic structure calculations deliver energetic and molecular parameters for all species involved in the reaction which are further utilized in multichannel–multiwell Rice–Ramsperger–Kassel–Marcus Master Equation (RRKM-ME) computations[53,54] to predict temperature- and pressure-dependent rate constants. For barrierless reaction entrance channels, the variable reaction coordinate – transition state theory (VRC-TST)[55,56] is utilized with energy evaluation at the CASPT2 level of theory. In cases where VRC-TST calculations are impractical, phase space theory[57] is employed where the potential power exponents and prefactors are fit to match the high-pressure limit rate constants to those of the closest analogous prototype reactions for which the rate constants are available.

A kinetics data gap still exists for the reactions described in the present *Account*. The experimental data overviewed here provide relatively little kinetic information and the kinetic data are generally lacking in the literature. The void can be filled by theoretical studies but accurate theoretical kinetics calculations of

reaction rate constants, relative pathway contributions, and product branching fractions in barrierless multichannel/multiwell radical–radical reactions is an extremely challenging and time-consuming task. Among the systems overviewed in the present *Account*, this task was accomplished so far only for the methyl–cyclopentadienyl,[58] cyclopentadienyl–cyclopentadienyl,[59] and propargyl–benzyl[1] reactions and, very recently, for propargyl–fulvenallenyl.[60] Future theoretical calculations providing quantitative assessment of total reaction rate constants and relative pathway contributions under standardized conditions which would provide valuable mechanistic insight are strongly appealed for.

Overall, this approach provides a directed synthesis of aromatics through radical–radical reactions under well-defined temperature and pressure profiles with radicals generated pyrolytically from thermally labile precursors. Residence times within the reactor can be tuned through the variation of the length of the pyrolysis tube, the backing pressure, and the selection of the noble gas with shortest residence times of a few tens of microseconds. The isomer-selective identification of aromatics along with their branching ratios represents an unprecedented advantage compared to hard electron impact (EI) ionization, which not only leads to fragmentation of the parent, but also excludes identification of distinct structural isomers. The relative yields of different products measured experimentally can then be compared with the yield obtained in the CFD/kinetic modeling.

3. RESULTS AND DISCUSSION

The radical–radical reactions involving C1 to C13 hydrocarbon radicals act as fundamental benchmarks for the gas-phase synthesis of small aromatics carrying up to three rings (Figures 3–4). Through the combination of molecular beam experiments with electronic structure calculations, six versatile mechanisms are revealed, which allow for the preparation of truly complex PAHs beyond anthracene and phenanthrene in the gas phase: **P**ropargyl **A**ddition – **B**enz**A**nnulation (**PABA**), **M**ethyl **A**ddition – **R**ing **E**xpansion (**MARE**), **C**yclo**P**entadienyl **A**ddition – **N**aphthylization (**CPAN**), **F**ulvenallenyl **A**ddition – **C**yclization – **A**romatization (**FACA**), **B**enzyl **A**ddition – **A**romatization (**BAA**), and **P**henyl **A**ddition – **P**entacyclization (**PAP**).

3.1. Propargyl Addition – BenzAnnulation (PABA)

The propargyl–benzyl system leading to naphthalene via annulation of a six-membered ring represents a prototype reaction of the **PABA** mechanism coupled with a hydrogen-atom-assisted isomerization (Figure 6b).[1] This reaction is initiated by the rapid, barrierless recombination of the open-shell reactants at their radical centers, with the resonance stabilization of the propargyl radical resulting in additions to the C1 (head) and C3 (tail) carbon atoms. These reaction intermediates undergo multiple isomerization steps via, e.g., ring closure and hydrogen migration with the reaction sequence eventually leading to atomic hydrogen loss accompanied by formation of methylene-indanyl radicals ($C_{10}H_9$). Their fast secondary isomerization through, e.g., hydrogen shifts, ring openings, and ring closures followed by another atomic hydrogen loss forms predominantly benzofulvene and naphthalene. Kinetic modeling suggests that the majority of naphthalene is generated via a hydrogen-assisted isomerization of benzofulvene. Although the reaction commences with a barrierless radical–radical recombination, the overall formation of naphthalene plus two hydrogen atoms is endoergic by 10 kJ mol^{-1} with isomerization barriers and/or exit transition states ranging at least 35 kJ mol^{-1} above the separated reactants. Consequently, this pathway solely operates in high temperature environments. This concept was expanded via the propargyl – 1-/2-naphthylmethyl system by preparing anthracene and phenanthrene (Figure 6c).[35,61] Since the **PABA** mechanism involves two reactive C3 moieties—one reactive moiety at each radical—technically, the propargyl–propargyl self-reaction[31] (Figure 6a) can be considered as the simplest reaction forming a six-membered ring from two reactive C3 units. Our investigation exposed three entrance channels through recombination of the radical centers: C1 (head) plus C3 (tail), C1 (head) plus C1 (head), and C3 (tail) plus C3 (tail) leading to acyclic C_6H_6 intermediates (1,5-hexadiyne, 1,2,3,4-hexatetraene, 1,2-hexadiene-5-yne), which eventually isomerize to fulvene (C_6H_6). This intermediate then undergoes ring expansion followed by a rapid hydrogen migration to benzene, which can be stabilized by a third body collider.

Overall, **PABA** signifies a ring-annulation to an existing six-membered aromatic ring through the reaction of the propargyl radical with a benzyl moiety of a PAH via hydrogen-assisted isomerization of fulvenes (Figure 6). **PABA** provides a template for the formation of more complex PAHs such as $C_{18}H_{12}$ isomers carrying four six-membered rings in the **C3+C14** system via the reaction of propargyl with ylomethyl ($–CH_2•$) substituted anthracene and phenanthrene molecules leading to the gas phase formation of helicenes, acenes, and phenacenes along with their

fulvene-type intermediates. Therefore, this versatile mechanism can lead to multi-benzene-ringed aromatics through benzannulation in high temperature combustion flames as well as in circumstellar envelopes of carbon rich stars and planetary nebulae.

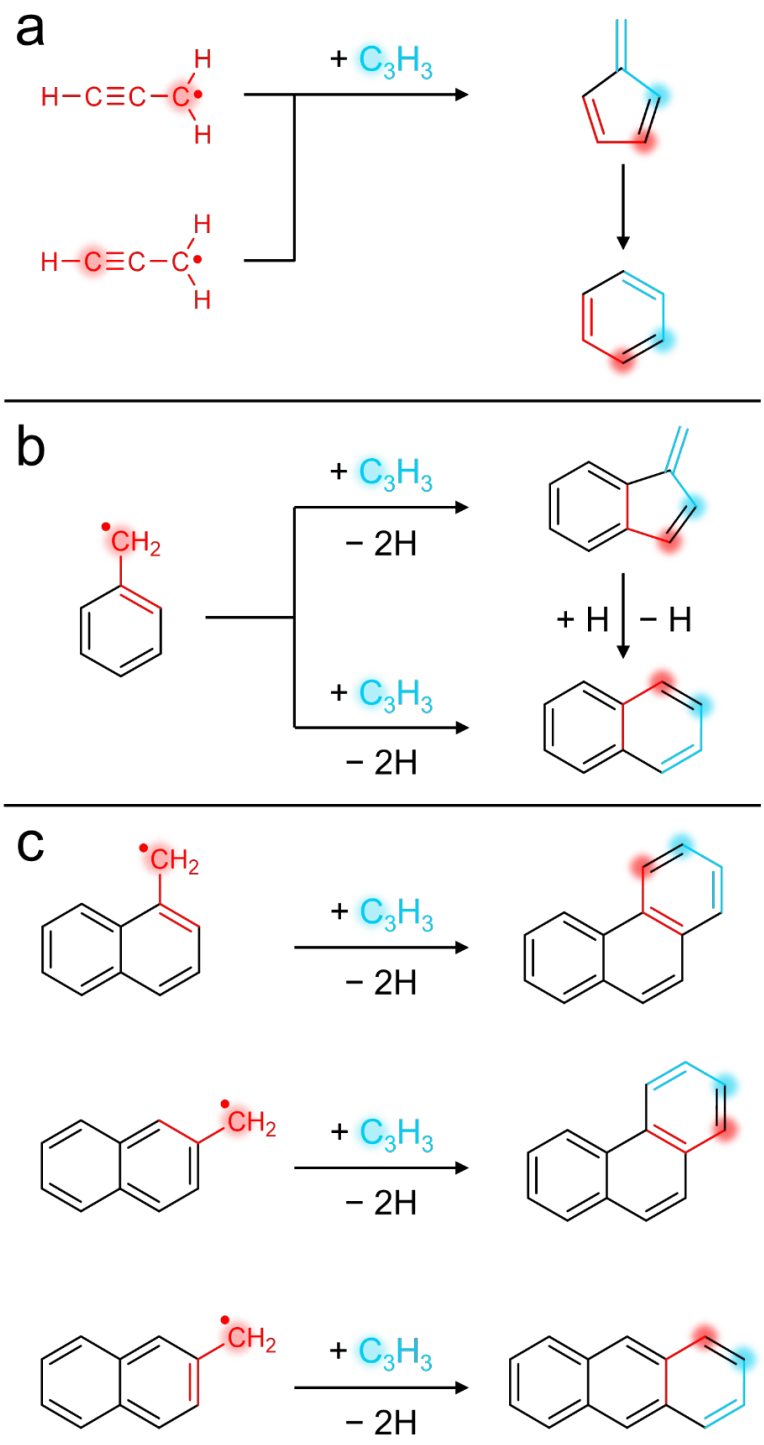

Figure 6. Major reaction pathways to aromatics via **P**ropargyl **A**ddition – **B**enz**A**nnulation (**PABA**). The red and blue colors indicate which portions of the products are due to each reactant, and the combination centers of each reactant are represented by red and blue circles.

3.2. Methyl Addition – Ring Expansion (MARE)

The methyl–cyclopentadienyl system leading to benzene signifies the simplest representative of the **MARE** mechanism which effectively converts a five-membered ring to a six-membered benzene ring (**C1+C5**) (Figure 7).[2] This concept of expanding a five-membered ring to a benzene moiety is versatile and can be systematically expanded from methyl–cyclopentadienyl (**C1+C5**) to methyl – 1-indenyl (**C1+C9**)[32] and methyl–fluorenyl (**C1+C13**)[34] synthesizing naphthalene and anthracene/phenanthrene, respectively. The prototype methyl–cyclopentadienyl system (Figure 7a) is initiated by a barrierless radical–radical reaction resulting in a carbon–carbon bond coupling. Two competing reaction sequences form fulvene and benzene with the actual branching ratios determined by the reactor temperature and pressure. The pathway to benzene involves atomic hydrogen loss of the addition intermediate followed by extensive isomerization (hydrogen shift, cyclization, ring opening) terminated by a hydrogen atom loss. The reaction sequence to fulvene involves first two successive hydrogen shifts and only then two stepwise hydrogen atom losses. In strong analogy to **PABA**, the fulvene moiety can be converted to a benzene ring through hydrogen assisted isomerization. Note that although the initial radical–radical recombination has no entrance barrier, the overall endoergicity of the reaction (+ 103 kJ mol^{-1}) and the fact that multiple transition states are located above the energy of the separated reactants blocks this reaction from operating at lower temperatures of cold molecular clouds; high-temperature environments are required.

The mechanism to formation of naphthalene in the methyl – 1-indenyl (**C1+C9**) reaction (Figure 7b) mirrors the elementary steps in the methyl–cyclopentadienyl (**C1+C5**) system, with barrierless addition of the methyl radical to the radical center of 1-indenyl at the C1/C3 atom followed by hydrogen loss, intermediate isomerizations, and hydrogen atom loss to the benzene moiety. However, whereas in the **C1+C5** system all five carbon atoms of the cyclopentadienyl radical are chemically equivalent, the C1/C3 and C2 carbon atoms are distinct in the cyclopentadienyl moiety of the 1-indenyl radical. Here, a second pathway involves the addition of methyl to the C2 carbon atom (Figure 7c) which has a lower spin density (0.20) compared to C1/C3 (0.50). This addition is followed by an equivalent multi-step route to naphthalene as in the C1/C3 addition case. Considering the distinct spin densities and the statistical factor, addition to C1/C3 is favored by a factor of 4 compared to C2. Note that an isomer of naphthalene, benzofulvene, can

also be produced, which can be converted by a hydrogen-assisted isomerization to naphthalene as operating in the **PABA** pathway.

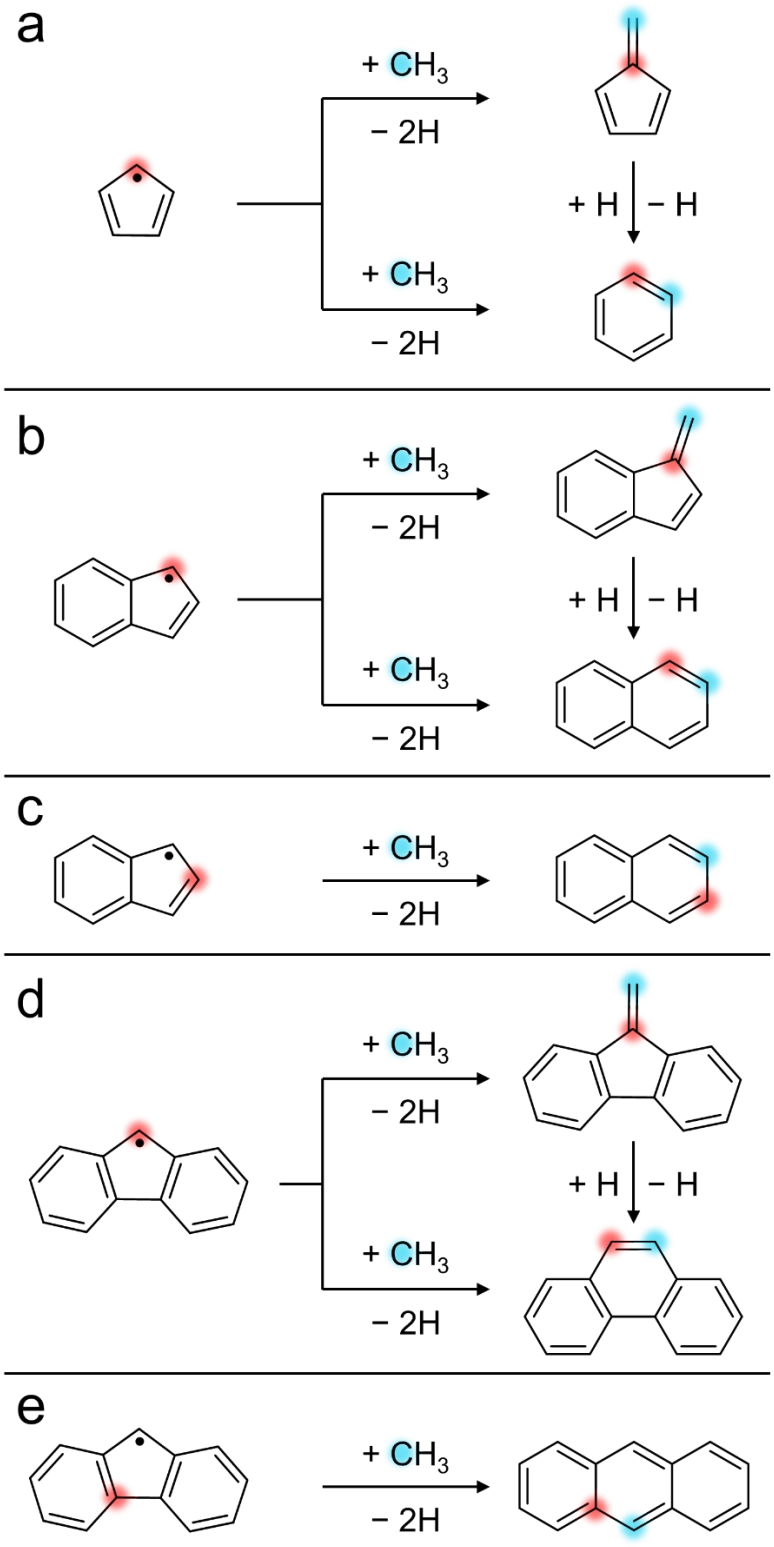

Figure 7. Major reaction pathways to aromatics via **M**ethyl **A**ddition – **R**ing **E**xpansion (**MARE**). The combination centers of each reactant are represented by red and blue circles.

Finally, the methyl–fluorenyl (**C1+C13**) reaction synthesizing at least anthracene and phenanthrene reflects the methyl – 1-indenyl system where radical addition may occur in different positions. The formation of phenanthrene is initiated through barrierless radical–radical recombination between methyl and the highest spin density (0.62) C9 carbon of fluorenyl (Figure 7d). The remaining reaction pathway is parallel to the methyl – 1-indenyl system involving hydrogen loss, hydrogen migration, three-membered ring cyclization, ring opening, and finally another atomic hydrogen loss to phenanthrene. Dibenzofulvene can also be formed and converted to phenanthrene through hydrogen assisted isomerization. It was found that the methyl radical can also add to the C4a carbon of fluorenyl (Figure 7e), which has a low spin density of only 0.13, eventually leading to anthracene via hydrogen loss, three-membered ring cyclization, ring opening, and hydrogen atom ejection.

Overall, **MARE** effectively converts a cyclopentadienyl moiety through reaction with methyl to a benzene moiety at high temperatures. This versatile ring expansion holds common features in all reactions investigated: a barrierless addition of the methyl radical to the unpaired electron of the cyclopentadienyl moiety, hydrogen losses, isomerization via hydrogen shift, ring formation to unusual bicyclic reaction intermediates carrying a five- and three-membered ring, ring opening, and—as an indirect route—the hydrogen-assisted isomerization of fulvene-type intermediates (Figure 7).

3.3. CycloPentadienyl Addition – Naphthylization (CPAN)

The cyclopentadienyl self-reaction (**C5+C5**) forming naphthalene embodies the prototype of the **CPAN** mechanism (Figure 8).[2] This mechanism de facto transforms spiroaromatic reaction intermediates accessed by a barrierless recombination of two cyclopentadienyl moieties to a naphthalene moiety. This versatile concept can be systematically expanded from **C5+C5** to the cyclopentadienyl – 1-indenyl (**C5+C9**) system accessing anthracene and phenanthrene thus converting any five-membered ring to a 10π aromatic naphthalene building block.[36] In detail, the cyclopentadienyl self-reaction commences with the formation of *cis*/*trans*-9,10-dihydrofulvalene ($C_{10}H_{10}$) via recombination of the reactants with their radical centers resulting in the formation of a carbon–carbon single bond. This intermediate loses a hydrogen atom from the newly formed bridge which then isomerizes to a highly strained tricyclic intermediate with connected five-,

three-, and five-membered rings (5-3-5) (Figure 8a), in which one five-membered and one three-membered ring are fused via a spiro carbon atom (5-3). This structure then rearranges via ring opening to a spiroaromatic intermediate, which fuses a five- and six-membered ring (5-6). The latter isomerized then to a bicyclic $C_{10}H_{11}$ intermediate which carries the naphthalene moiety prior to losing a hydrogen atom from the bridging carbon atom leading to aromatization and formation of naphthalene.

The versatility of the aforementioned mechanism is reflected in the cyclopentadienyl – 1-indenyl (**C5+C9**) system. Classically, recombination of both radical reactants with the radical centers located at the C1 carbon atoms leads to the 1-(cyclopenta-2,4-dien-1-yl)-1*H*-indene intermediate ($C_{14}H_{12}$) via carbon–carbon single bond coupling (Figure 8b). The latter undergoes ring closure to a tetracyclic (6-**5-3-5**) spirane intermediate, which isomerizes through ring opening to a tricyclic spirane structure (6-**6-5**); the numbers in bold represent the equivalent spirane substructures in the cyclopentadienyl self-reaction (**C5+C5**). Eventually, this spirane doublet radical undergoes ring contraction followed by isomerization to a singly hydrogenated phenanthrene radical intermediate ($C_{14}H_{11}$) which then emits a hydrogen atom from the bridging carbon atom to form phenanthrene. However, our discovery of anthracene reveals an unusual reaction pathway that involves a barrierless combination of cyclopentadienyl with the 1-indenyl radical at the C2 carbon atom adjacent to the traditional C1 radical center with a lower spin density (0.38) (Figure 8c). This pathway to 2-(cyclopenta-2,4-dien-1-yl)-2*H*-indene ($C_{14}H_{12}$) follows addition to the carbon atom with the lower spin density in analogy to the cyclopentadienyl self-reaction (**C5+C5**) as outlined above. This intermediate can eject a hydrogen atom followed by isomerization to a spirane radical succeeded by ring opening to yet another spirane radical, which then ring opens to a singly hydrogenated anthracene species. The latter loses a hydrogen atom to form the anthracene molecule.

Overall, the recombination of two cyclopentadienyl moieties within the framework of the **CPAN** mechanism as demonstrated for the **C5+C5** and **C5+C9** systems leads via exotic spiroaromatic intermediates to a naphthalene backbone with pathways following the classical route through recombination of the carbon-centered radicals at the carbon atoms of the highest spin densities, but also through a non-classical path via addition to the carbon atom holding the lower spin density. Once again, although the initial radical–radical recombinations are barrierless, the

endoergicity of these reactions from 38 to 87 kJ mol^{-1} suggests that **CPAN** only operates at high temperatures.

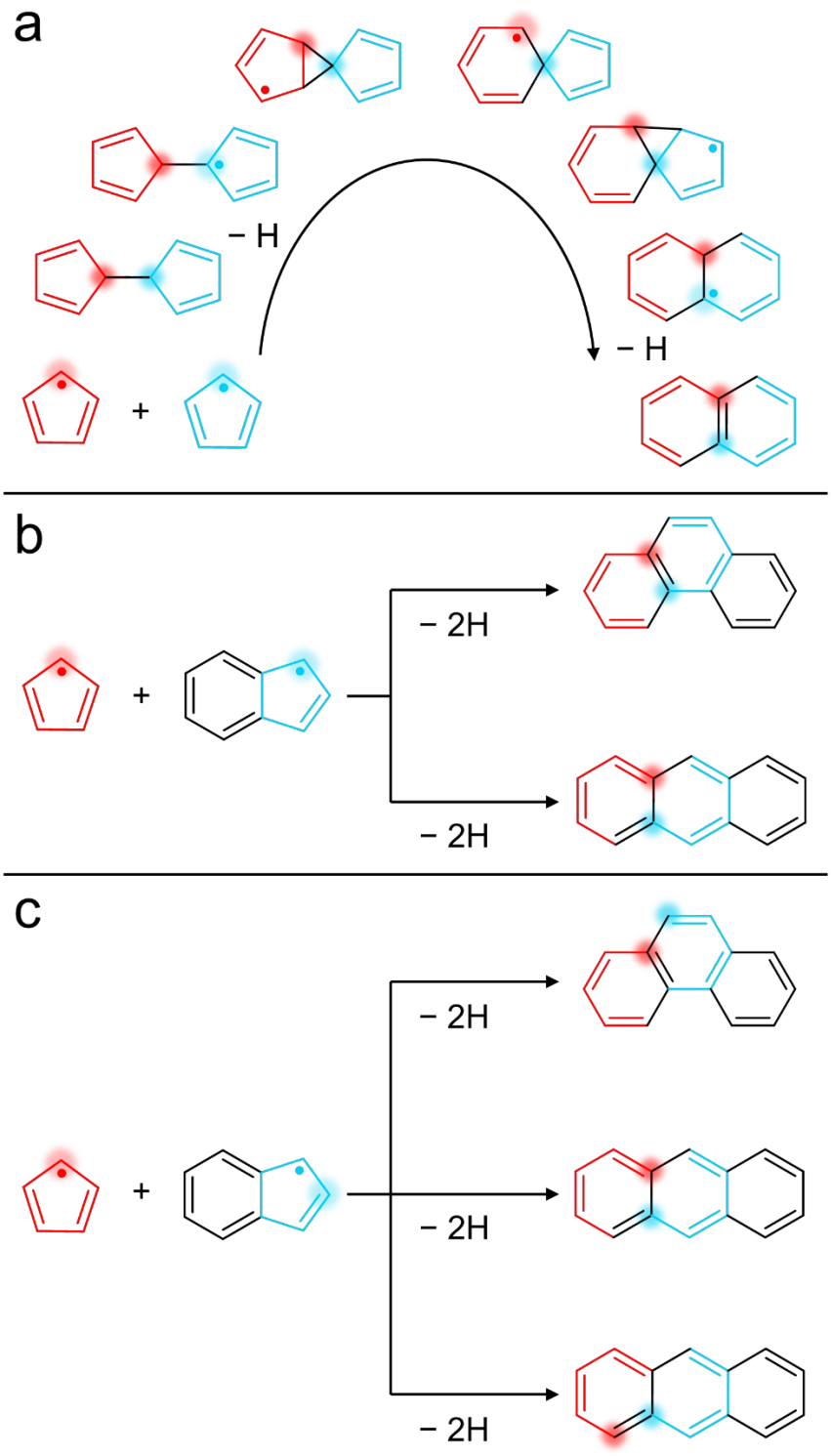

Figure 8. Major reaction pathways to aromatics via **C**yclo**P**entadienyl **A**ddition – **N**aphthylization (**CPAN**). The red and blue colors indicate which portions of the products are due to each reactant, and the combination centers of each reactant are represented by red and blue circles.

3.4. Fulvenallenyl Addition – Cyclization – Aromatization (FACA)

The **FACA** mechanism (**C3+C7**) facilitates molecular mass growth processes through the reaction of two RSFRs—propargyl and fulvenallenyl—accessing naphthalene as well as its azulene isomer (Figure 9a).[33] The complex reactivity of fulvenallenyl with propargyl is driven by eight distinct entrance channels along with 5-methylene-5H-indene ($C_{10}H_8$) and fulvalene ($C_{10}H_8$) intermediates which can be converted to naphthalene as well as its azulene isomer via hydrogen-assisted isomerization. The elucidated reaction mechanism affords a versatile concept introducing an azulene moiety, i.e. a seven-membered ring adjacent to a five-membered ring, into polycyclic aromatic systems via molecular mass growth processes. Note that the fulvenallenyl radical self-reaction,[62] while similar to **FACA**, does not lead to formation of a seven-membered ring. Commencing with the bimolecular reaction of a PAH-embedded benzene ring with a methylidyne radical (CH), a six-membered ring can be effectively converted into a fulvenallene moiety as long as the embedded benzene ring has three adjacent hydrogen atoms demonstrated in the crossed molecular beam reaction of benzene with methylidyne (CH).[63] A hydrogen atom loss from the exocyclic allenic functional group leads to the PAH-embedded fulvenallenyl unit, which can then react with a propargyl radical to the azulene moiety incorporated in an aromatic system. These seven-membered rings are a critical prerequisite of exotic saddle-shaped aromatic systems with both positive and negative curvature of the carbon backbone.[64]

3.5. Benzyl Addition – Aromatization (BAA)

The traditional viewpoint of the benzyl radical self-reaction (**C7+C7**) (Figure 9b) suggests a recombination on the ground state singlet potential energy surface with their radical centers at the ylomethyl moieties leading to 1,2-diphenylethane ($C_6H_5CH_2CH_2C_6H_5$), which can lose successively two hydrogen atoms from the bridging group forming trans-stilbene ($C_6H_5CHCHC_6H_5$).[3] The acyclic C6 moiety comprising the olefinic –CH=CH– group and the adjacent carbon atom of the phenyl rings are the backbone of the successive cyclization process. Here, a hydrogen loss from one of the *ortho* carbon atoms of the phenyl group leads to the *trans*-stilbenyl ($C_6H_4CHCHC_6H_5$, $C_{14}H_{11}$) radical, which then undergoes ring closure and finally hydrogen atom loss resulting in aromatization and an isomer-selective synthesis of phenanthrene on the singlet surface.

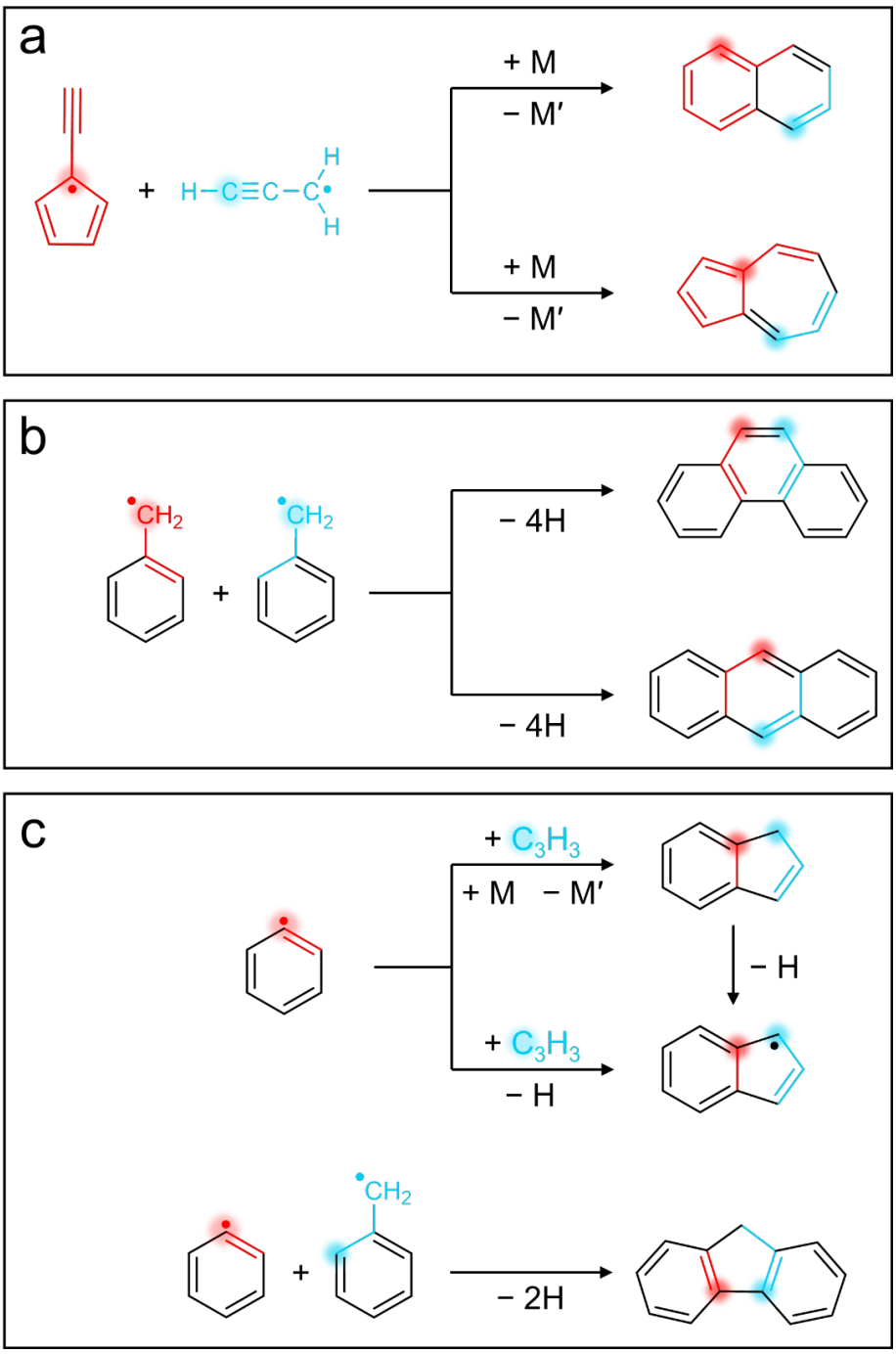

Figure 9. Major reaction pathways to aromatics via **(a) F**ulvenallenyl **A**ddition – **C**yclization – **A**romatization (**FACA**), **(b) B**enzyl **A**ddition – **A**romatization (**BAA**), and **(c) P**henyl **A**ddition – **P**entacyclization (**PAP**). The red and blue colors indicate which portions of the products are due to each reactant, and the combination centers of each reactant are represented by red and blue circles.

However, the aforementioned mechanism failed to account for the experimentally observed anthracene isomer. Electronic structure calculations revealed that both benzyl radicals can also recombine on the triplet surface (a^3A) via [3+3] cycloaddition leading to triplet 4a,8a,9,10-tetrahydroanthracene ($C_{14}H_{14}$). This intermediate, which does not exist on the singlet surface, is formed via a single collision between two benzyl radicals via cycloaddition and involves a significant reorganization of the σ- and π-electron densities. Three successive atomic hydrogen losses commencing with triplet 4a,8a,9,10-tetrahydroanthracene yield anthracene. The overall reactivity is influenced by the cone-of-acceptance of the benzyl radical leading to the initial collision complexes forming eventually phenanthrene versus anthracene on the singlet and triplet surface, respectively. While the cycloaddition is geometrically constrained and governed by low impact parameters, the preferred synthesis of phenanthrene over anthracene is driven by facile recombination and carbon-carbon bond coupling of the benzyl radicals at their ylomethyl moieties.

Overall, the **BAA** mechanism effectively operates via reactive **C3+C3** centers as does the **PABA** mechanism. However, whereas **PABA** solely proceeds on the ground state singlet surface, excited state dynamics via [3+3] cycloaddition also operate for **BAA**. These excited state dynamics on the triplet surface producing eventually anthracene defy conventional wisdom that PAH formation via radical–radical reactions solely operate on electronic ground state surfaces through recombination of the doublet reactants at their radical centers. The versatility of **BAA** suggests that any aromatic radical carrying a benzyl moiety may react with a benzyl structure in a second aromatic radical synthesizing new multi-ringed structures such as three-ring carbon skeletons from mono-ringed radical moieties at high-temperature conditions. While the triplet state mechanism is essential in the **BAA** mechanism, it does not appear to be competitive for the other reactions, e.g., benzyl + propargyl.[1]

3.6. Phenyl Addition – Pentacyclization (PAP)

The propargyl–phenyl[37] and benzyl–phenyl[4] systems signify the two simplest representatives of the **P**henyl **A**ddition – **P**entacyclization (**PAP**) mechanism (Figure 9c). These **C3+C6** and **C7+C6** systems are distinct from the reaction mechanisms discussed above since they involve the reaction of an odd-carbon-numbered radical with an even-carbon-numbered radical. Hence, this mechanism does not lead to the preparation of a six-membered ring, but rather a five-membered

ring annulated by one (**C3+C6**) and two (**C7+C6**) six-membered rings via molecular mass growth processes involving reactive **C2** (phenyl) and **C3** (propargyl; benzyl) units. The **C3+C6** reaction to indene can be initiated via a classical recombination of the phenyl radical center with that of the propargyl radical at the C1 or C3 carbon atom leading to 3-phenyl-1-propyne (C_9H_8) and phenylallene (C_9H_8), respectively. Isomerization via hydrogen migration and cyclization leads to indene, which can either be stabilized by a third body reaction or lose a hydrogen atom forming the indenyl radical. Overall, this reaction is barrierless, exoergic, and all transition states involved reside below the energy of the separated reactants, i.e. the critical prerequisites to operate in low temperature environments such as in cold molecular clouds or hydrocarbon rich atmospheres of planets and their moons.

The formation of *9H*-fluorene is driven by an unconventional mechanism via addition of the phenyl radical to the *ortho* position of the benzyl radical, but not by a classical radical–radical recombination at the radical centers, which produces diphenylmethane ($C_6H_5CH_2C_6H_5$) via third body stabilization. This pathway produces a 1-(6-methylenecyclohexa-2,4-dienyl)benzene intermediate through a barrierless recombination of an RSFR with an AR at the carbon atom adjacent to the traditional C1 radical center followed by two sequential atomic hydrogen losses via a 9a,9-dihydrofluorenyl radical to *9H*-fluorene. Although the reaction proceeds barrierlessly and is exoergic, the transition state of the final hydrogen loss resides above the energy of the separated reactants; hence, this reaction only operates at high-temperature environments.

Overall, the **PAP** mechanism effectively proceeds via annulation of a five-membered ring to an existing phenyl radical and affords a potential route to add five-membered rings to any aryl radical with a hydrogen atom on the *ortho* position of the radical center on the six-membered ring. The **C7+C6** system provides evidence that the reaction of two radicals does not necessarily proceed via recombination of their classical radical centers with the highest spin density as revealed for the **MARE** and **CPAN** mechanisms as well.

4. SUMMARY AND OUTLOOK

Radical–radical reactions of RSFRs and/or ARs described in this *Account* established a fundamental mechanism to molecular mass growth processes to PAHs carrying up to three rings. ReTOF-MS and PEPICO coupled with tunable vacuum ultraviolet single photon ionization and

electronic structure calculations provided a versatile, isomer-selective approach to identify the reaction products in a molecular beam and to classify these reactions into six reaction mechanisms (Table 1):

Table 1. Schematic mechanisms and summary of the reactions discussed within this *Account*.

	Name	Reaction	Rings	Mechanistic Notes	Schematics
PABA	Propargyl Addition BenzAnnulation	3+3 3+7 3+11	1 2 3	Propargyl head or tail addition Fulvene intermediates	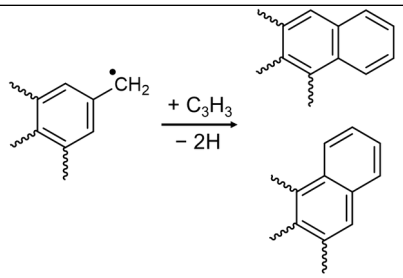
MARE	Methyl Addition Ring Expansion	1+5 1+9 1+13	1 2 3	Fulvene intermediates Three-membered ring intermediates	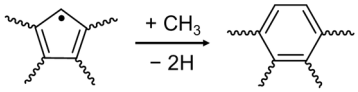
CPAN	CycloPentadienyl Addition Naphthylization	5+5 5+9	2 3	Low or high spin density addition Spiroaromatic Intermediates	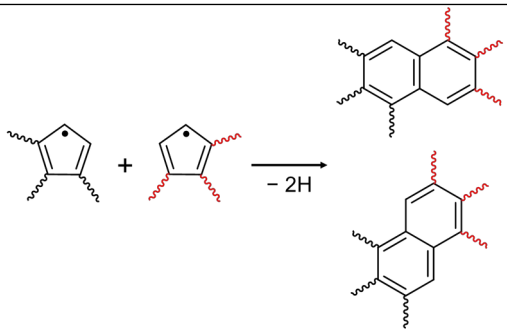
FACA	Fulvenallenyl Addition Cyclization Aromatization	3+7	2	Propargyl tail addition Methyleneindene intermediates	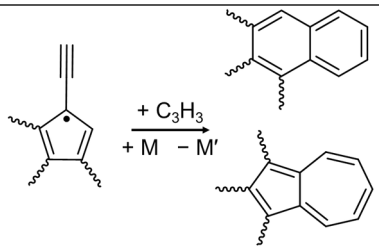
BAA	Benzyl Addition Aromatization	7+7	2	Singlet surface recombination Triplet surface cycloaddition	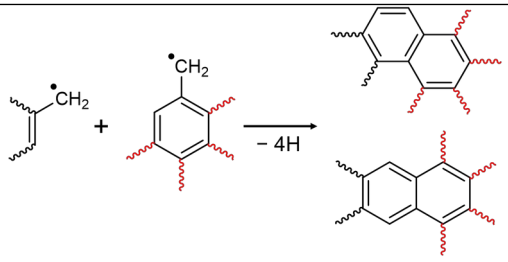

PAP	Phenyl Addition Pentacyclization	6+3 6+7	2 3	Low spin density addition	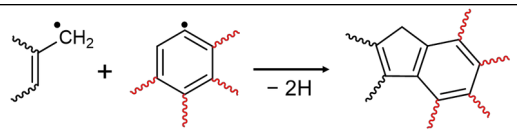

1. Propargyl **A**ddition – **B**enz**A**nnulation (**PABA**)

2. Methyl **A**ddition – **R**ing **E**xpansion **(MARE)**

3. Cyclo**P**entadienyl **A**ddition – **N**aphthylization **(CPAN)**

4. Fulvenallenyl **A**ddition – **C**yclization – **A**romatization (**FACA**)

5. Benzyl **A**ddition – **A**romatization **(BAA)**

6. Phenyl **A**ddition – **P**entacyclization (**PAP**)

These reaction mechanisms explore molecular mass growth of aromatic molecules by systematically increasing the molecular weight of the reactants in steps of **C2** and **C4** units to reveal unconventional concepts beyond the classical perception that radical–radical reactions are initiated through formation of a carbon–carbon single bond when the carbon-centered radicals with their highest spin density recombine. Unconventional cycloadditions on excited state triplet surfaces, additions of radicals to carbon-centered radicals with low spin densities, spiroaromatic and fulvene-type intermediates, and highly strained bicyclic reaction intermediates challenge traditional paradigms. Finally, it should be highlighted that apart from **FACA**, the remaining reaction mechanisms only operate at high temperatures due to high barriers or overall highly endoergic reactions. Therefore, these molecular mass growth pathways might be central to circumstellar environments of carbon-rich stars and planetary nebulae, but they play no role in the gas phase of cold molecular clouds where temperatures as low as 10 K dominate.[65]

With reaction pathways via radical–radical reactions to simple aromatic systems now understood (Figures 6–9), future experiments are aimed to more complex systems synthesizing and identifying aromatics beyond three rings. As the number of aromatic rings increases, so does the number of structural isomers which can be formed in these reactions. However, as the number of structural isomers increases, the adiabatic ionization energies of the PAHs and the shapes of the PIEs, which are distinct for smaller PAHs, can be very similar and even identical in the most unfavorable case. Therefore, alternative detection schemes to probe PAHs formed in a chemical

microreactor, offering higher structural sensitivity, are required. PEPICO represents such an alternative. The gas-phase preparation of anthracene and phenanthrene via **MARE** from the methyl–fluorenyl system[34] demonstrates the unique potential of an isomer-selective PAH detection exploiting fragment-free photoionization coupled with PIE curves and ms-TPE spectra, which should be applicable to more complex radical–radical reactions. It further delivers a strategy to explore chemical reactions of ARs and RSFRs under high-temperature environments of relevance to synthetic and materials chemistry and astrophysical processes leading eventually to carbonaceous nanostructures like fullerenes, nanocages, and nanotubes thus deciphering the aromatic universe we live in.

NOTES

The author declares no competing financial interest.

BIOGRAPHY

Shane J. Goettl earned his B.S. in chemistry at the University of Wisconsin–Stevens Point in 2018 and is currently pursuing a Ph.D. in physical chemistry at the University of Hawaii at Manoa. His research focuses on molecular mass growth processes to polycyclic aromatic hydrocarbons in extreme environments and experimental dynamics of organosilicon bimolecular reactions.

Musahid Ahmed is a senior scientist at Lawrence Berkeley National Laboratories. He received his Ph.D. in 1989 at Cambridge University and pursued postdoctoral fellowships at Leicester, Gottingen, and Manchester. He started probing water cluster beams with vacuum ultraviolet radiation at the Daresbury synchrotron which led him to join Berkeley lab in 1995 to pursue a career in using synchrotron radiation to probe gas, interfacial, and condensed phase chemical dynamics with molecular and aerosol beams.

Alexander M. Mebel received his Ph.D. in physical chemistry at Kurnakov's Institute of General and Inorganic Chemistry. After postdoctoral appointments in Germany, Japan, and USA, his first faculty position was at the Institute of Atomic and Molecular Sciences (Academia Sinica, Taiwan), and in 2003 he joined the Department of Chemistry and Biochemistry of Florida International University, where he is currently Professor of Chemistry and Chair (since 2024). He was elected Fellow of the Combustion Institute in 2021. His current research interests include theoretical quantum chemical studies of mechanisms, kinetics, and dynamics of elementary chemical reactions related to combustion, atmospheric, and interstellar chemistry.

Ralf I. Kaiser received his Ph.D. from the University of Münster in 1994, conducted postdoctoral work at UC Berkeley, and performed his habilitation at the University Chemnitz and Institute of Atomic and Molecular Sciences (Academia Sinica, Taiwan). He joined the Department of Chemistry at the University of Hawaii at Manoa in 2002, where he is currently Professor of Chemistry and Director of the W. M. Keck Research Laboratory in Astrochemistry. He was elected

Fellow of the Royal Astronomical Society, the Royal Society of Chemistry, the American Physical Society, the American Association for the Advancement of Science, the Institute of Physics (UK), and of the American Chemical Society. His group pioneered the exploitation of crossed molecular beams and molecular beams in conjunction with tunable vacuum ultraviolet light to unravel elementary reactions fundamental to the chemistry of the interstellar medium and circumstellar envelopes.

ACKNOWLEDGMENTS

The preparation of this *Account* was supported by the US Department of Energy, Basic Energy Sciences (DE-FG02-03ER15411). MA gratefully acknowledges support from the Director, Office of Energy Research, Office of Basic Energy Sciences, Chemical Sciences Division of the U.S. Department of Energy under contract No. DE-AC02-05CH11231, through the Gas Phase Chemical Physics program. SJG, MA, AMM, and RIK acknowledge and thank the coauthors and collaborators that contributed to the published work mentioned in this *Account*.

REFERENCES

(1) He, C.; Kaiser, R. I.; Lu, W.; Ahmed, M.; Krasnoukhov, V. S.; Pivovarov, P. S.; Zagidullin, M. V.; Azyazov, V. N.; Morozov, A. N.; Mebel, A. M. Unconventional gas-phase preparation of the prototype polycyclic aromatic hydrocarbon naphthalene ($C_{10}H_8$) via the reaction of benzyl (C_7H_7) and propargyl (C_3H_3) radicals coupled with hydrogen-atom assisted isomerization. *Chem. Sci.* **2023**, *14*, 5369.

(2) Kaiser, R. I.; Zhao, L.; Lu, W.; Ahmed, M.; Zagidullin, M. V.; Azyazov, V. N.; Mebel, A. M. Formation of benzene and naphthalene through cyclopentadienyl-mediated radical–radical reactions. *J. Phys. Chem. Lett.* **2022**, *13*, 208.

(3) Kaiser, R.; Zhao, L.; Lu, W.; Ahmed, M.; Krasnoukhov, V. S.; Azyazov, V. N.; Mebel, A. M. Unconventional excited-state dynamics in the concerted benzyl (C_7H_7) radical self-reaction to anthracene ($C_{14}H_{10}$). *Nat. Commun.* **2022**, *13*, 1.

(4) He, C.; Kaiser, R. I.; Lu, W.; Ahmed, M.; Pivovarov, P. S.; Kuznetsov, O. V.; Zagidullin, M. V.; Mebel, A. M. Unconventional pathway in the gas-phase synthesis of *9H*-fluorene ($C_{13}H_{10}$) via the radical–radical reaction of benzyl (C_7H_7) with phenyl (C_6H_5). *Angew. Chem., Int. Ed.* **2023**, *62*, e202216972.

(5) Garden, A. Singular substance found in a coal tar apparatus. *Ann. Philos.* **1820**, *15*, 74.

(6) Tielens, A. G. G. M. Interstellar polycyclic aromatic hydrocarbon molecules. *Annu. Rev. Astron. Astrophys.* **2008**, *46*, 289.

(7) Kaiser, R. I.; Parker, D. S. N.; Mebel, A. M. Reaction dynamics in astrochemistry: Low-temperature pathways to polycyclic aromatic hydrocarbons in the interstellar medium. *Annu. Rev. Phys. Chem.* **2015**, *66*, 43.

(8) Siegmann, K.; Sattler, K.; Siegmann, H. C. Clustering at high temperatures: carbon formation in combustion. *J. Electron Spectrosc. Relat. Phenom.* **2002**, *126*, 191.

(9) Draine, B. T. Interstellar dust grains. *Annu. Rev. Astron. Astrophys.* **2003**, *41*, 241.

(10) Villaume, A.; Conroy, C.; Johnson, B. D. Circumstellar dust around AGB stars and implications for infrared emission from galaxies. *Astrophys. J.* **2015**, *806*, 82.

(11) Edwards, N. T. Polycyclic aromatic hydrocarbons (PAH's) in the terrestrial environment—A review. *J. Environ. Qual.* **1983**, *12*, 427.

(12) Nisbet, I. C. T.; LaGoy, P. K. Toxic equivalency factors (TEFs) for polycyclic aromatic hydrocarbons (PAHs). *Regul. Toxicol. Pharmacol.* **1992**, *16*, 290.

(13) Kalpana, M. S.; Babu, E. V. S. S. K.; Mani, D.; Tripathi, R. P.; Bhandari, N. Polycyclic aromatic hydrocarbons in the Mukundpura (CM2) Chondrite. *Planet. Space Sci.* **2021**, *198*, 105177.

(14) Rhee, Y. M.; Lee, T. J.; Gudipati, M. S.; Allamandola, L. J.; Head-Gordon, M. Charged polycyclic aromatic hydrocarbon clusters and the galactic extended red emission. *Proc. Natl. Acad. Sci. U. S. A.* **2007**, *104*, 5274.

(15) Duley, W. W. Polycyclic aromatic hydrocarbons, carbon nanoparticles and the diffuse interstellar bands. *Faraday Discuss.* **2006**, *133*, 415.

(16) Ricks, A. M.; Douberly, G. E.; Duncan, M. A. The infrared spectrum of protonated naphthalene and its relevance for the unidentified infrared bands. *Astrophys. J.* **2009**, *702*, 301.

(17) Wenzel, G.; Gong, S.; Xue, C.; Changala, P. B.; Holdren, M. S.; Speak, T. H.; Stewart, D. A.; Fried, Z. T. P.; Willis, R. H. J.; Bergin, E. A. et al. Discovery of the seven-ring polycyclic

aromatic hydrocarbon cyanocoronene ($C_{24}H_{11}CN$) in GOTHAM observations of TMC-1. *Astrophys. J.* **2025**, *984*, L36.
(18) Johansson, K. O.; Head-Gordon, M. P.; Schrader, P. E.; Wilson, K. R.; Michelsen, H. A. Resonance-stabilized hydrocarbon-radical chain reactions may explain soot inception and growth. *Science* **2018**, *361*, 997.
(19) Naraoka, H.; Takano, Y.; Dworkin, J. P.; Oba, Y.; Hamase, K.; Furusho, A.; Ogawa, N. O.; Hashiguchi, M.; Fukushima, K.; Aoki, D. et al. Soluble organic molecules in samples of the carbonaceous asteroid (162173) Ryugu. *Science* **2023**, *379*, eabn9033.
(20) Zeichner, S. S.; Aponte, J. C.; Bhattacharjee, S.; Dong, G.; Hofmann, A. E.; Dworkin, J. P.; Glavin, D. P.; Elsila, J. E.; Graham, H. V.; Naraoka, H. et al. Polycyclic aromatic hydrocarbons in samples of Ryugu formed in the interstellar medium. *Science* **2023**, *382*, 1411.
(21) Shukla, B.; Koshi, M. A novel route for PAH growth in HACA based mechanisms. *Combust. Flame* **2012**, *159*, 3589.
(22) Frenklach, M.; Wang, H. Detailed modeling of soot particle nucleation and growth. *Symp. (Int.) Combust.* **1991**, *23*, 1559.
(23) Yang, T.; Kaiser, R. I.; Troy, T. P.; Xu, B.; Kostko, O.; Ahmed, M.; Mebel, A. M.; Zagidullin, M. V.; Azyazov, V. N. HACA's heritage: a free-radical pathway to phenanthrene in circumstellar envelopes of asymptotic Giant Branch Stars. *Angew. Chem., Int. Ed.* **2017**, *129*, 4586.
(24) Parker, D. S. N.; Zhang, F.; Kim, Y. S.; Kaiser, R. I.; Landera, A.; Kislov, V. V.; Mebel, A. M.; Tielens, A. G. G. M. Low temperature formation of naphthalene and its role in the synthesis of PAHs (polycyclic aromatic hydrocarbons) in the interstellar medium. *Proc. Natl. Acad. Sci. U. S. A.* **2012**, *109*, 53.
(25) Shukla, B.; Susa, A.; Miyoshi, A.; Koshi, M. Role of phenyl radicals in the growth of polycyclic aromatic hydrocarbons. *J. Phys. Chem. A* **2008**, *112*, 2362.
(26) Xiong, S.; Li, J.; Wang, J.; Li, Z.; Li, X. Kinetic study of the formation of triphenylene from the condensation of $C_{12}H_{10} + C_6H_5$. *Comput. Theor. Chem.* **2012**, *985*, 1.
(27) Zhao, L.; Prendergast, M. B.; Kaiser, R. I.; Xu, B.; Ablikim, U.; Ahmed, M.; Sun, B. J.; Chen, Y. L.; Chang, A. H. H.; Mohamed, R. K. Synthesis of polycyclic aromatic hydrocarbons by phenyl addition–dehydrocyclization: The third way. *Angew. Chem., Int. Ed.* **2019**, *131*, 17603.
(28) Doddipatla, S.; Galimova, G. R.; Wei, H.; Thomas, A. M.; He, C.; Yang, Z.; Morozov, A. N.; Shingledecker, C. N.; Mebel, A. M.; Kaiser, R. I. Low-temperature gas-phase formation of indene in the interstellar medium. *Sci. Adv.* **2021**, *7*, eabd4044.
(29) Zhang, F.; Kaiser, R. I.; Kislov, V. V.; Mebel, A. M.; Golan, A.; Ahmed, M. A VUV photoionization study of the formation of the indene molecule and Its isomers. *J. Phys. Chem. Lett.* **2011**, *2*, 1731.
(30) Goettl, S. J.; Tuli, L. B.; Turner, A. M.; Reyes, Y.; Howlader, A. H.; Wnuk, S. F.; Hemberger, P.; Mebel, A. M.; Kaiser, R. I. Gas-phase synthesis of coronene through stepwise directed ring annulation. *J. Am. Chem. Soc.* **2023**, *145*, 15443.
(31) Zhao, L.; Lu, W.; Ahmed, M.; Zagidullin, M. V.; Azyazov, V. N.; Morozov, A. N.; Mebel, A. M.; Kaiser, R. I. Gas-phase synthesis of benzene via the propargyl radical self-reaction. *Sci. Adv.* **2021**, *7*, eabf0360.

(32) Zhao, L.; Kaiser, R.; Lu, W.; Xu, B.; Ahmed, M.; Morozov, A. N.; Mebel, A. M.; Howlader, A. H.; Wnuk, S. F. Molecular mass growth through ring expansion in polycyclic aromatic hydrocarbons via radical–radical reactions. *Nat. Commun.* **2019**, *10*, 1.
(33) Li, W.; Yang, J.; Zhao, L.; Couch, D.; Marchi, M. S.; Hansen, N.; Morozov, A. N.; Mebel, A. M.; Kaiser, R. I. Gas-phase preparation of azulene ($C_{10}H_8$) and naphthalene ($C_{10}H_8$) via the reaction of the resonantly stabilized fulvenallenyl ($C_7H_5^{\cdot}$) and propargyl ($C_3H_3^{\cdot}$) radicals. *Chem. Sci.* **2023**, *14*, 9795.
(34) Goettl, S. J.; Turner, A. M.; Krasnoukhov, V. S.; Azyazov, V. N.; Kanayama, K.; Hemberger, P.; Mebel, A. M.; Kaiser, R. I. Gas-phase synthesis of anthracene and phenanthrene via radical-radical reaction induced ring expansions. *Sci. Adv.* **2025**, *11*, eadv0692.
(35) Wang, C. Y.; Zhao, L.; Kaiser, R. I. Gas-phase preparation of the 14π Hückel polycyclic aromatic anthracene and phenanthrene isomers ($C_{14}H_{10}$) via the Propargyl Addition–BenzAnnulation (PABA) mechanism. *ChemPhysChem* **2024**, *25*, e202400151.
(36) He, C.; Kaiser, R. I.; Lu, W.; Ahmed, M.; Reyes, Y.; Wnuk, S. F.; Mebel, A. M. Exotic reaction dynamics in the gas-phase preparation of anthracene ($C_{14}H_{10}$) via spiroaromatic radical transients in the indenyl–cyclopentadienyl radical–radical reaction. *J. Am. Chem. Soc.* **2023**, *145*, 3084.
(37) Yang, Z.; Galimova, G. R.; He, C.; Goettl, S. J.; Paul, D.; Lu, W.; Ahmed, M.; Mebel, A. M.; Li, X.; Kaiser, R. I. Gas-phase formation of the resonantly stabilized 1-indenyl (C_9H_7) radical in the interstellar medium. *Sci. Adv.* **2023**, *9*, eadi5060.
(38) Guan, Q.; Urness, K. N.; Ormond, T. K.; David, D. E.; Barney, E. G.; Daily, J. W. The properties of a micro-reactor for the study of the unimolecular decomposition of large molecules. *Int. Rev. Phys. Chem.* **2014**, *33*, 447.
(39) Zagidullin, M. V.; Kaiser, R. I.; Porfiriev, D. P.; Zavershinskiy, I. P.; Ahmed, M.; Azyazov, V. N.; Mebel, A. M. Functional relationships between kinetic, flow, and geometrical parameters in a high-temperature chemical microreactor. *J. Phys. Chem. A* **2018**, *122*, 8819.
(40) Chai, J.-D.; Head-Gordon, M. Systematic optimization of long-range corrected hybrid density functionals. *J. Chem. Phys.* **2008**, *128*.
(41) Chai, J.-D.; Head-Gordon, M. Long-range corrected hybrid density functionals with damped atom–atom dispersion corrections. *Phys. Chem. Chem. Phys.* **2008**, *10*, 6615.
(42) Goerigk, L.; Grimme, S. Efficient and accurate double-hybrid-meta-GGA density functionals—Evaluation with the extended GMTKN30 database for general main group thermochemistry, kinetics, and noncovalent interactions. *J. Chem. Theory Comput.* **2011**, *7*, 291.
(43) Adler, T. B.; Knizia, G.; Werner, H.-J. A simple and efficient CCSD (T)-F12 approximation. *J. Chem. Phys.* **2007**, *127*, 221106.
(44) Knizia, G.; Adler, T. B.; Werner, H.-J. Simplified CCSD (T)-F12 methods: Theory and benchmarks. *J. Chem. Phys.* **2009**, *130*, 054104.
(45) Dunning Jr., T. H. Gaussian basis sets for use in correlated molecular calculations. I. The atoms boron through neon and hydrogen. *J. Chem. Phys.* **1989**, *90*, 1007.
(46) Peterson, K. A.; Adler, T. B.; Werner, H.-J. Systematically convergent basis sets for explicitly correlated wavefunctions: The atoms H, He, B–Ne, and Al–Ar. *J. Chem. Phys.* **2008**, *128*, 084102.

(47) Curtiss, L. A.; Raghavachari, K.; Redfern, P. C.; Rassolov, V.; Pople, J. A. Gaussian-3 (G3) theory for molecules containing first and second-row atoms. *J. Chem. Phys.* **1998**, *109*, 7764.
(48) Curtiss, L. A.; Redfern, P. C.; Raghavachari, K. Gaussian-4 theory. *J. Chem. Phys.* **2007**, *126*.
(49) Curtiss, L. A.; Raghavachari, K.; Redfern, P. C.; Baboul, A. G.; Pople, J. A. Gaussian-3 theory using coupled cluster energies. *Chem. Phys. Lett.* **1999**, *314*, 101.
(50) Celani, P.; Werner, H.-J. Multireference perturbation theory for large restricted and selected active space reference wave functions. *J. Chem. Phys.* **2000**, *112*, 5546.
(51) Miller, J. A.; Klippenstein, S. J.; Georgievskii, Y.; Harding, L. B.; Allen, W. D.; Simmonett, A. C. Reactions between resonance-stabilized radicals: Propargyl + allyl. *J. Phys. Chem. A* **2010**, *114*, 4881.
(52) Morozov, A. N.; Mebel, A. M. Theoretical study of the reaction mechanism and kinetics of the phenyl + propargyl association. *Phys. Chem. Chem. Phys.* **2020**, *22*, 6868.
(53) Georgievskii, Y.; Miller, J. A.; Burke, M. P.; Klippenstein, S. J. Reformulation and solution of the master equation for multiple-well chemical reactions. *J. Phys. Chem. A* **2013**, *117*, 12146.
(54) Georgievskii, Y.; Klippenstein, S. J. *Master Equation System Solver [MESS]*, 2016.3.23, **2015**; see https://tcg.cse.anl.gov/papr.
(55) Georgievskii, Y.; Klippenstein, S. J. Transition state theory for multichannel addition reactions: multifaceted dividing surfaces. *J. Phys. Chem. A* **2003**, *107*, 9776.
(56) Harding, L. B.; Georgievskii, Y.; Klippenstein, S. J. Predictive theory for hydrogen atom–hydrocarbon radical association kinetics. *J. Phys. Chem. A* **2005**, *109*, 4646.
(57) Klippenstein, S. J.; Cline, J. I. Classical phase space theory for product state distributions with application to the *v–j* vector correlation. *J. Chem. Phys.* **1995**, *103*, 5451.
(58) Krasnoukhov, V. S.; Porfiriev, D. P.; Zavershinskiy, I. P.; Azyazov, V. N.; Mebel, A. M. Kinetics of the CH_3 + C_5H_5 reaction: A theoretical study. *J. Phys. Chem. A* **2017**, *121*, 9191.
(59) Long, A. E.; Merchant, S. S.; Vandeputte, A. G.; Carstensen, H.-H.; Vervust, A. J.; Marin, G. B.; Van Geem, K. M.; Green, W. H. Pressure dependent kinetic analysis of pathways to naphthalene from cyclopentadienyl recombination. *Combust. Flame* **2018**, *187*, 247.
(60) Morozov, A. N.; Pratali Maffei, L.; Mebel, A. M. Rate constants of the fulvenallenyl recombination with propargyl and its role in PAH formation: A theoretical and kinetic modeling study. *Phys. Chem. Chem. Phys.* **2025**, *27*, 11577.
(61) Wu, M.; Liu, Z.; Chu, Z.; Wu, X.; Huang, J.; Yang, J.; Yang, B.; Zhang, F. A weight growth route from 2-naphthylmethyl radical to tricyclic aromatics. *Proc. Combust. Inst.* **2024**, *40*, 105535.
(62) Li, W.; Wu, M.; Wang, C.; Huang, J.; Yang, J.; Xu, M.; Zhang, F.; Yang, T.; Zhao, L. Unconventional pathway for the gas-phase formation of 14π-PAHs via self-reaction of the resonantly stabilized radical fulvenallenyl ($C_7H_5^{\cdot}$). *Chem. Sci.* **2025**, *16*, 7864.
(63) He, C.; Thomas, A. M.; Galimova, G. R.; Morozov, A. N.; Mebel, A. M.; Kaiser, R. I. Gas-phase formation of fulvenallene (C_7H_6) via the Jahn–Teller distorted tropyl (C_7H_7) radical intermediate under single-collision conditions. *J. Am. Chem. Soc.* **2020**, *142*, 3205.

(64) Ma, J.; Fu, Y.; Dmitrieva, E.; Liu, F.; Komber, H.; Hennersdorf, F.; Popov, A. A.; Weigand, J. J.; Liu, J.; Feng, X. Helical nanographenes containing an azulene unit: Synthesis, crystal structures, and properties. *Angew. Chem., Int. Ed.* **2020**, *59*, 5637.
(65) Davis, D. N. The spectrum of β Pegasi. *Astrophys. J.* **1947**, *106*, 28.
(66) Zhao, L.; Yang, T.; Kaiser, R. I.; Troy, T. P.; Xu, B.; Ahmed, M.; Alarcon, J.; Belisario-Lara, D.; Mebel, A. M.; Zhang, Y. et al. A vacuum ultraviolet photoionization study on high-temperature decomposition of JP-10 (exo-tetrahydrodicyclopentadiene). *Phys. Chem. Chem. Phys.* **2017**, *19*, 15780.
(67) Biswas, S.; Paul, D.; Dias, N.; Lu, W.; Ahmed, M.; Pantoya, M. L.; Kaiser, R. I. Efficient oxidative decomposition of jet-fuel exo-tetrahydrodicyclopentadiene (JP-10) by aluminum nanoparticles in a catalytic microreactor: An online vacuum ultraviolet photoionization study. *J. Phys. Chem. A* **2024**, *128*, 1665.